

## Real-world outdoor air exposure effects in a model of the human airway epithelium – A comparison of healthy and asthmatic individuals using a mobile laboratory setting

Pavel Rossner<sup>a,\*</sup>, Helena Libalova<sup>a,1</sup>, Tereza Cervena<sup>a</sup>, Michal Sima<sup>a</sup>, Zuzana Simova<sup>a</sup>, Kristyna Vrbova<sup>a</sup>, Antonin Ambroz<sup>a</sup>, Zuzana Novakova<sup>a</sup>, Fatima Elzeinova<sup>a</sup>, Anezka Vimrova<sup>a</sup>, Lubos Dittrich<sup>b</sup>, Michal Vojtisek<sup>b</sup>, Martin Pechout<sup>b</sup>, Michal Vojtisek-Lom<sup>b</sup>

<sup>a</sup> Department of Toxicology and Molecular Epidemiology, Institute of Experimental Medicine CAS, Prague, Czech Republic

<sup>b</sup> Faculty of Mechatronics, Informatics and Interdisciplinary Studies, Technical University of Liberec, Liberec, Czech Republic

### ARTICLE INFO

Edited by Professor Bing Yan

#### Keywords:

outdoor air pollution  
lung tissue model  
asthma  
real-world exposure  
air-liquid interface

### ABSTRACT

We developed a mobile laboratory allowing field exposure of lung tissue models to ambient air at localities with various pollution sources (Background, Industrial, Traffic, Urban) in different seasons (summer/fall/winter). In samples originating from healthy and asthmatic individuals, we assessed the parameters of toxicity, lipid peroxidation and immune response; we further performed comprehensive monitoring of air pollutants at sampling sites. We measured lactate dehydrogenase (LDH) and adenylate kinase (AK) production and transepithelial electrical resistance (TEER), analyzed 15-F<sub>2t</sub>-isoprostane (IsoP) and a panel of 20 cytokines/chemokines/growth factors. In the ambient air, we detected particulate matter (PM), and other relevant chemicals (benzene, benzo[a]pyrene (BaP), NO<sub>x</sub>). In the Traffic locality, we found very high concentrations of ultrafine particles and NO<sub>x</sub> and observed low TEER values in the exposed samples, indicating significant traffic-related toxicity of the ambient air. In the Urban locality, sampled in winter, we observed high PM and BaP levels. We found lower AK levels in samples from healthy individuals exposed in this locality than in the asthmatic samples. In the samples from the Industrial locality, sampled in summer, we detected higher concentrations of TNF $\alpha$ , MIP-1 $\alpha$ , Eotaxin, GRO $\alpha$ , GM-CSF, IL-6 and IL-7 than in the Urban locality samples. We hypothesize that pollen or other plant-related components of the ambient air were responsible for this response. In conclusion, our data proved the feasibility of our mobile laboratory for field measurements of the biological response of lung tissue models exposed to ambient air, reflecting not only the levels of toxic compounds, but also season-specific parameters.

### 1. Introduction

Ambient air pollution significantly affects human health worldwide. While chronic exposure to air pollutants increases the incidence of cardiovascular, respiratory or neurodegenerative disorders, short-term acute exposure exacerbates asthma and chronic obstructive lung disease (COPD) (Yatera and Nishida, 2024). Importantly, outdoor air pollution has been classified as carcinogenic to humans (IARC Working Group on the Evaluation of Carcinogenic Risks to Humans, 2016). It is

estimated that particulate matter of aerodynamic diameter < 2.5  $\mu$ m (PM<sub>2.5</sub>), an important constituent of air pollution, contributes to excess deaths of up to 8 million/year (the estimates differ depending on the source) (Pozzer et al., 2023).

Air pollution is characterized by its complexity: it consists of a mixture of particulate matter (PM) of various sizes, chemical compounds bound to it and gaseous components. The combination of these constituents as well as their physical and chemical properties predetermine the health impacts of air pollution. These specific characteristics

**Abbreviations:** AK, adenylate kinase; ALI, air-liquid interface; BALF, bronchoalveolar lavage fluid; BaP, benzo[a]pyrene; CHMI, Czech Hydrometeorological Institute; COPD, chronic obstructive lung disease; EEPS, Engine Exhaust Particle Sizer; IPF, idiopathic pulmonary fibrosis; IsoP, 15-F<sub>2t</sub>-isoprostane; NO<sub>x</sub>, nitrogen oxides; PM, particulate matter; TEER, transepithelial electrical resistance; VOC, volatile organic compound.

\* Correspondence to: Videnska 1083, Prague 14200, Czech Republic.

E-mail address: [pavel.rossner@iem.cas.cz](mailto:pavel.rossner@iem.cas.cz) (P. Rossner).

<sup>1</sup> These authors contributed equally to this work

<https://doi.org/10.1016/j.ecoenv.2024.117495>

Received 12 September 2024; Received in revised form 26 November 2024; Accepted 4 December 2024

Available online 7 December 2024

0147-6513/© 2024 The Author(s). Published by Elsevier Inc. This is an open access article under the CC BY-NC license (<http://creativecommons.org/licenses/by-nc/4.0/>).

complicate the *in vitro* research of the mechanisms of ambient air toxicity. Traditionally, research of outdoor air pollution exposure health consequences has been performed in human populations, laboratory animals or in *in vitro* cell models, each of these approaches having its specific drawbacks. While human studies allow the results relevant to real-life scenarios to be obtained, they are bound by strict ethical regulations. This is also true, although to a lesser extent, for laboratory animal investigations. However, some species-specific differences may complicate extrapolation of these results to the human organism. Finally, *in vitro* cell model studies have mostly been limited to tests of separate components of air pollution (particles, or organic/inorganic extracts from particles) (Chen et al., 2018; Hanzalova et al., 2010; Líbalová et al., 2021; Rahmatinia et al., 2022), thus omitting interaction between the air pollution components, that may have fundamental impacts on the biological activity of air pollution.

Over the years, attempts have been made to address the drawbacks of *in vitro* exposure to air pollution and to construct systems allowing exposure to all components of polluted air (referred to as complete pollution). Aside from commercial instruments, various in-house apparatuses have been developed (Rossner et al., 2021), that were often used to evaluate the toxicity of engine emissions, but also to other aerosols/gases (Guénette et al., 2022; Wang et al., 2019). However, a very limited number of studies focused specifically on the effects of environmental (ambient) air pollution (Bisig et al., 2018; Costabile et al., 2023; Gualtieri et al., 2018; Santoro et al., 2024; Vizuete et al., 2015).

In *in vitro* testing, the selection of the model system is another important consideration. Traditionally, submerged cell cultures consisting of a single cell type, often of cancer origin, have been used. This approach has several limitations, including the fact that it does not allow complete pollution tests, as well as the specific response of the tumor cells, particularly on the molecular level, thus requiring cautious conclusions when assessing e.g. gene expression changes (Lujan et al., 2019).

With the above-mentioned limitations in mind, we designed the current study that focuses on characterization of the biological response of the human primary cells of the airway epithelium (MucilAir™), an *in vitro* cell model grown on the air-liquid interface (ALI). The cell cultures, obtained from both healthy and asthmatic human subjects, were exposed to ambient air in field conditions at four localities of the Czech Republic differing in concentrations and characteristics of air pollutants [Background, Industrial, Traffic, Urban] as well as meteorological conditions. We used our previously developed compact exposure chamber (Vojtisek-Lom et al., 2019) and modified it so that it can be used as a mobile laboratory.

The aim of our study was to develop an ALI exposure system that serves as a mobile laboratory and that can be used, after meeting certain technical requirements, to assess the molecular response of lung tissue models to ambient air pollution in virtually any locality. We further focused on the identification of a possible different biological response in lung tissue samples originating from healthy and asthmatic subjects.

## 2. Materials and methods

### 2.1. Cell cultures, exposure conditions and localities

In all experiments, the model of human airway epithelium (MucilAir™; Epithelix Sàrl, Geneva, Switzerland) was used. The model was described in detail in our previous study (Rossner et al., 2019). In brief, MucilAir™ is a bronchial epithelial model reconstituted from primary human cells of healthy/asthmatic volunteers. For the study, samples derived from eight healthy donors (6 males, 2 females) and six asthma patients (1 male, 5 females) were used. The cell models were grown at ALI at 37 °C, 5 % CO<sub>2</sub>, and relative humidity > 90 % in 24-well format Transwell® cell culture inserts (Sigma-Aldrich, St Louis, MO, USA) in culture medium provided by the cell model manufacturer. Prior to using the cultures in experiments, they were grown for at least 3 weeks in the

laboratory and checked for their stability. The culture medium was replaced every 2–3 days and apical wash was performed every week to eliminate the accumulated mucus.

For the field experiments, a previously developed compact exposure chamber was used (Vojtisek-Lom et al., 2019). To address the specific requirements of this study, particularly to achieve mobility of the system, the equipment was further modified. The exposure boxes (up to two for exposed samples and two for the controls) were placed in a commercial small scale (40x35x45 cm inner dimensions) incubator, in which the pump, membrane humidifier and other accessories were incorporated, thus allowing sample conditioning to 5 % CO<sub>2</sub>, 37 °C, and relative humidity above 90 % (Figs. 1, 2, 3).

CO<sub>2</sub> was introduced at the inlet of the incubator for both sample types (controls and exposed) (Fig. 1, part A). Before the incubator inlet, a flow of approximately 3.3–3.6 lpm was diverted for an online analysis. A flow of around 0.4 lpm passed through the incubator wall (Fig. 1, part B), then through the heat exchanger (Fig. 1, part E), where it was heated to 37 °C, and through a membrane humidifier [model MH-110–12S-2 (Perma Pure LLC, Lakewood, NJ, USA)] (Fig. 1, part C). Deionized water was supplied from a water reservoir (Fig. 1, part D) installed on top of the humidifier. The relative humidity exceeded 90 % to ensure survival of the cells. On the humidifier outlet, a flow of 0.4 lpm was divided equally to two exposure chambers. A flow of 0.2 lpm passed through each of the four exposure chambers. The flow was controlled by rotameters with a needle valve and two air pumps (Fig. 1, part F). Each of the chambers was equipped with its own rotameter, plus two rotameters for CO<sub>2</sub> (one for each line) and two air pumps (one for each line). The control air flow was pre-controlled by rotameter placed on the incubator inlet.

This setting became the basis for the mobile laboratory, deployable either in a van or outdoors in a suitable shelter protected from the elements. The laboratory further included a small laminar flow box for manipulation with cell cultures, an additional incubator for housing exposure boxes that were not actively undergoing exposure, a freezer and pressure bottles with CO<sub>2</sub> (conditioning) and synthetic air (control sample) (Supplementary Figure 1A–D). As the equipment requires electric power, the mobile laboratory should ideally be located within reach of an electrical outlet. Optionally, we used a rechargeable battery of sufficient capacity to power the systems.

The field experiments were performed in four localities selected so that each represented specific ambient air characteristics (Fig. 4, Table 1). Kosetice (Background), was a control locality used as a background station of the Czech Hydrometeorological Institute (CHMI) (Supplementary Figure 2). The station is surrounded by fields/meadows/forests with no traffic/heating/industrial sources of pollution. Kvasiny (Industrial locality) was a town (population approx. 1700) with industrial production (automotive, wood processing/painting), where significant pollution of volatile organic compounds was expected (Supplementary Figure 3). The specific location of the station in the

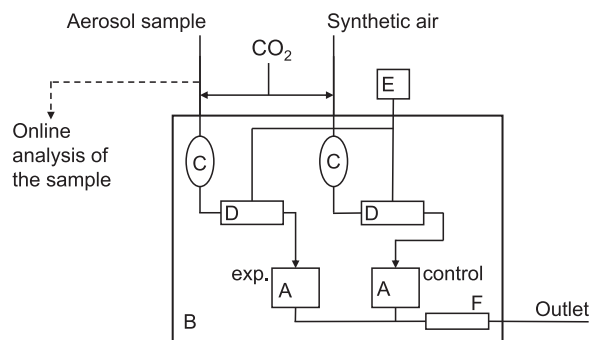


**Fig. 1.** Development of the exposure system: a schema of the modified incubator. A. Exposure chamber; B. Commercial incubator; C. Humidifier; D. Deionized water reservoir; E. Heat exchanger; F. Flow control and air pumps.



**Fig. 2.** Development of the exposure system: a commercial incubator housing exposure chambers and other equipment.

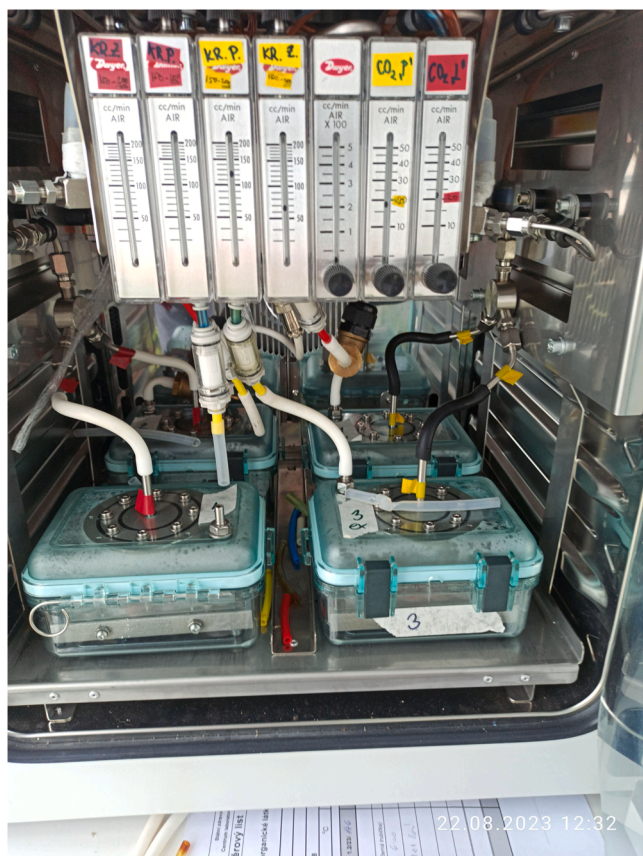


**Fig. 3.** Development of the exposure system: details of the exposure boxes in which cell cultures were placed.

town was selected following consultations with local inhabitants with knowledge of possible hotspots for air pollution. In the capital city of Prague (Traffic locality), a traffic hotspot at a 6-lane road with an average number of 100,000 passing cars/day was selected (Supplementary Figure 4). The city of Ostrava (population approx. 290,000) (Urban locality) represented a locality with a combination of traffic/industrial/heating air pollution (Supplementary Figure 5). The Ostrava region is a known hotspot of the Czech Republic with high concentrations of air pollutants (Rossner et al., 2015).

To simulate a potential scenario of human exposure to ambient air across the selected localities, emphasizing repeated exposures, the experiments were carried out over a five-day period. Each day followed this exposure regimen: 2-hour ambient air exposure, 2-hour resting period in the incubator, followed by another 2-hour exposure (Fig. 5). Control samples underwent the same pattern but were exposed to control air (Synthetic Air, Linde plc, Dublin, Ireland). Prior to exposure to both ambient and control air (at time point T0), we collected cell medium (basal medium and apical wash) and measured TEER to capture data from the cells unaffected by handling or exposure. Subsequently, after each exposure session, the cells were housed overnight for the next day's exposure and in the morning, the basal cell medium was changed.

## 2.2. Online air pollutant analysis

Total number concentrations of particles, including volatiles, were measured in all locations by a condensation particle counter (UF-CPC 200, Palas) with a 50 % counting efficiency (d50) at 5 nm.

Particle size distributions in 32 channels over the 5.6–560 nm range, classified by electric mobility diameter, were measured with a fast electric mobility particle sizer (Engine Exhaust Particle Sizer, EEPS), in all locations except the Background location, where the concentrations were deemed to be too low and close to the detection limit.

Particle mass concentrations in PM2.5 and PM10 categories was measured by gravimetry at Background and Urban sites and by online measurements at the Traffic hot spot; at the Industrial location only PM10 concentrations (gravimetrically assessed) were obtained.

According to the expected pollutants of concern, volatile organic compounds were measured at the Industrial location, nitrogen oxides (NOx) were measured at the Traffic hotspot, and particle-bound benzo [a]pyrene (BaP) was measured at the Urban mixed sources site. The overview of the measurements is shown in Table 1.

The results provided by the EEPS included concentration ( $\#/cm^3$ ) as a function of time measured in 32 output size channels, and particle size. The detection range of particles diameter of these channels was from 6.04 nm to 523.3 nm. The data were summed across the whole day to show the size distribution. Another set of data provided by the EEPS was the total concentration of particles ( $\#/cm^3$ ) as a function of time. These data were used to show the total concentration of particles through the whole set of exposures for each of the localities. The EEPS scans every second and these data were averaged to get the concentration values for every 60 seconds of exposure.

## 2.3. Meteorological conditions

For further characterization of the parameters that may have affected exposure experiments, meteorological conditions (minimum/maximum/mean temperature, mean air humidity, precipitation, sunshine and mean wind speed) during the field campaigns were noted. The information was obtained from the website of the CHMI (<https://www.chmi.cz/historicka-data/pocasi/denni-data/Denni-data-dle-z.-123-1998-Sb>; in Czech). The data from the stations closest to the actual sampling sites were used (Supplementary File S1).

## 2.4. Transepithelial electrical resistance (TEER)

TEER measurements were conducted using an EVOM2 ohm meter (World Precision Instruments, Sarasota, FL, USA) paired with an STX2 electrode. This approach offers a quantitative, non-destructive method for assessing the integrity of tight junctions in cell culture models. All measurements were taken under sterile conditions to maintain cell culture viability. Prior to each measurement, 200  $\mu$ l of preheated MucilAir™ medium was added to the apical side of the inserts. The electrode was then equilibrated by rinsing with sterile phosphate-buffered saline (PBS) followed by preheated medium. Measurements were taken before exposure (T0) and on the fifth day prior to cell harvest

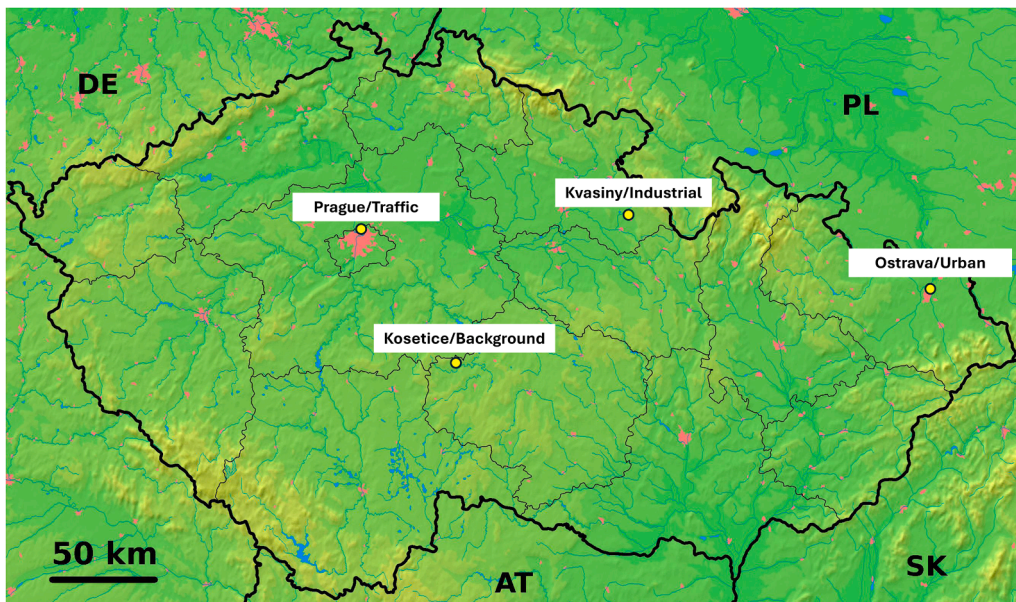


Fig. 4. A map of the Czech Republic with depicted localities of the field experiments.

Table 1  
Sampling locations characteristics.

Parameter	Locality (city/town name)			
	Kosetice	Kvasiny	Prague	Ostrava
Locality type	Background	Industrial	Traffic	Urban
GPS coordinates	49.5734883 N, 15.0808208E	50.2085744 N, 16.2553864E	50.1176100 N, 14.4614689E	49.8465047 N, 18.2836922E
Time of sampling (date)	4.8. – 8.8. 2023	21.8. – 25.8. 2023	18.9. – 22.9. 2023	2.12. – 6.12. 2023
Time of sampling (hours; each day)	6:30 – 16:00	6:30 – 16:00	6:30 – 16:00	6:30 – 16:00
PM10	yes	yes	yes	yes
PM2.5	yes	no	yes	yes
Particle number conc.	yes	yes	yes	yes
Size distribution	yes	yes	yes	yes
VOC	no	yes	no	yes
NOx	no	no	yes	no
BaP	no	no	no	yes

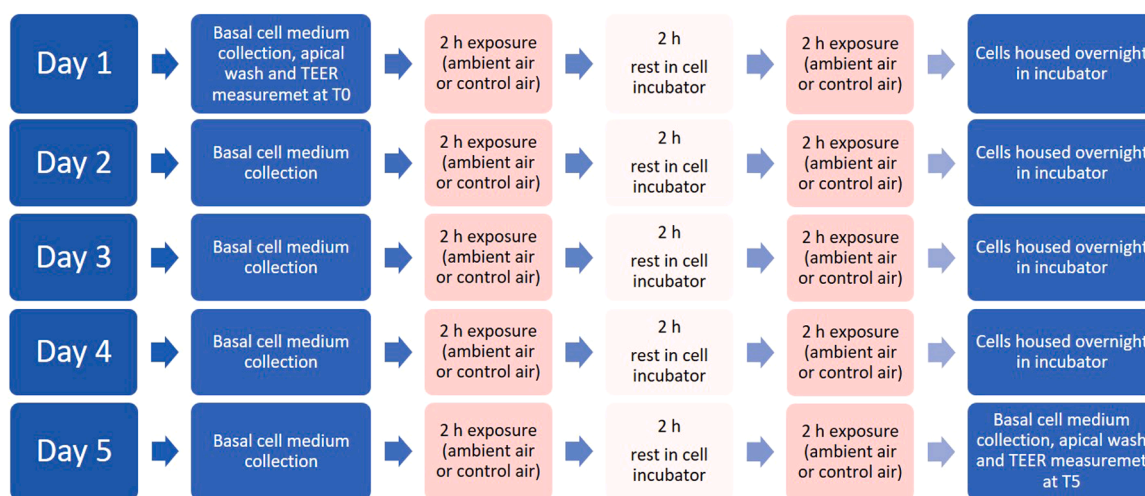


Fig. 5. The overview of the exposure experiments.

(T5). The resistance values were calculated using the formula: TEER (ohm\*cm<sup>2</sup>) = (resistance of the test tissue (ohm) - resistance value of the untreated membrane (ohm)) x surface area of the epithelium (cm<sup>2</sup>). Here, the resistance value of the untreated membrane was set at 100

ohm, and the epithelium surface area was 0.33 cm<sup>2</sup>.

## 2.5. Cytotoxicity measurements

Lactate dehydrogenase (LDH) and adenylate kinase (AK) activities were analyzed in the basal cell culture medium using the Cytotoxicity Detection Kit (Roche, Basel, Switzerland) and Adenylate Kinase Cytotoxicity Assay Kit (Abcam, Cambridge, UK), respectively. Both methods were performed according to the manufacturer's instructions with some modifications: each sample was analyzed in technical duplicate using 50  $\mu\text{L}$  sample/well. In the case of LDH, 50  $\mu\text{L}$  of the reaction mixture (Catalyst in  $\text{H}_2\text{O}$  + Dye solution) was added to each well; the samples were incubated for 30 minutes at 37 °C in the dark and for 30 minutes at room temperature (RT) in the dark. For AK, 50  $\mu\text{L}$  of the AK reaction mixture was added to each well; the samples were incubated for 15 minutes at RT in the dark. At the end, absorbance at 490 nm for LDH detection and luminescence for AK assay was measured by SpectraMax®M5e (Molecular Devices, San Jose, CA, USA). The final outcomes were expressed as the percentage of cytotoxicity relative to the positive control (1 % v/v Triton X-100, 1 h, and 37 °C).

## 2.6. Cytokine production

The production of selected cytokines, chemokines and growth factors (a complete list is indicated in Supplementary File S2) into the basal cell culture medium was assessed using The Human ProcartaPlex™ Mix & Match 22-plex (Thermo Fisher Scientific, Wilmington, DE, USA) according to the manufacturer's instructions. Briefly, 50  $\mu\text{L}$  of the Capture Bead Mix was added to each well of the 96-well plate. After a washing procedure using a Hand-Held Magnetic Plate Washer, 50  $\mu\text{L}$ /well of prepared standards and samples in technical duplicates were added and shook at 600 rpm for 2 hours at RT. After washing the plate, 25  $\mu\text{L}$ /well of the Biotinylated detection Antibody Mix was added and shook at 600 rpm for 30 minutes at RT. After another washing step, 50  $\mu\text{L}$ /well of Streptavidin-PE was added and shook at 600 rpm for 30 minutes at RT. After the final washing process, 120  $\mu\text{L}$  of reading buffer was added into each well and shook at 600 rpm for 5 minutes at RT before running the plate on the xMAP™ instrument BIOPLEX 200 System (Luminex, Austin, TX, USA). Data were analyzed in Bio-Plex Manager 6.0 (Bio-Rad Laboratories, Hercules, CA, USA).

## 2.7. 15-F<sub>2t</sub>-isoprostane detection

The concentration of 15-F<sub>2t</sub>-isoprostane (IsoP) in the basal cell culture medium was analyzed using the 8-isoprostane ELISA kit (Cayman Chemicals Company, Ann Arbor, MI, USA) according to the manufacturer's instructions. Calibration standards were prepared in the cell medium, each sample (50  $\mu\text{L}$ ) was analyzed in a technical duplicate and the absorbance was detected by SpectraMax®iD3 (Molecular Devices, San Jose, CA, USA) at 405 nm. Results were calculated based on the standard calibration curve with a detection range of 0.8 – 500 pg/mL.

## 2.8. Statistical analysis

MucilAir™ samples exposed to ambient air in each tested locality originated from either healthy donors (eight persons) or asthmatic donors (six persons, two technical replicates). Exposure of the control MucilAir™ samples to control air was performed simultaneously with the ambient air exposure using the same healthy/asthmatic samples. For the purpose of the statistical analysis, the control samples (separately for healthy and asthmatic) from all localities were pooled; each consisted of a total of thirty-two replicates. The parameters were compared using the Kruskal-Wallis non-parametric test with Dunn's (post-hoc) multiple comparison test in GraphPad Prism version 8 (GraphPad Software Inc., San Diego, CA, USA). Data were presented as boxplots. For the multiplex immunoassay, data were not examined for conditions where the result was calculated to be zero for more than five out of eight replicates or twenty out of thirty-two replicates, respectively. The statistically

significant difference between indicated pairs were denoted by asterisks (\* $p < 0.05$ , \*\* $p < 0.01$ , \*\*\* $p < 0.001$ ).

## 3. Results

### 3.1. Air pollution characterization, meteorological conditions

The field experiments were organized so that diverse types/concentrations of ambient air pollutants and meteorological conditions were evaluated. For general characterization of air pollution, particles in the ambient air were assessed. In all localities, PM10 concentrations ( $\mu\text{g}/\text{m}^3$ ), as well as particle number concentration ( $\#/\text{cm}^3$ ) and, except for the Background location, particle size distributions (dN/dlogDp [ $\#/\text{cm}^3$ ]) were analyzed (Table 1).

PM2.5 ( $\mu\text{g}/\text{m}^3$ ) was measured in all but the Industrial locality, where only daily PM10 values were available (the CHMI monitoring station was not equipped with the PM2.5 measuring system) (Table 1).

Depending on the source of pollution in the given locality, specific compounds were further monitored (Table 1). Thus, volatile organic compounds (VOC) were analyzed in the Industrial and Urban locality and information on benzene concentrations ( $\mu\text{g}/\text{m}^3$ ) were reported. NOx was measured in the Traffic locality and BaP was monitored in the Urban locality, in which high concentrations of this polycyclic aromatic hydrocarbon have been repeatedly found in the past. The contribution of these contaminants to the overall ambient air pollution in other localities was insignificant and thus they were not included in the battery of air pollution measurements.

The hourly concentrations of PM10/PM2.5 were determined during individual exposure periods as shown in Fig. 6A-D. Detailed information on particle number concentration ( $\#/\text{cm}^3$ ) and the size distribution (dN/dlogDp [ $\#/\text{cm}^3$ ]) is provided in Fig. 7A-D and Fig. 8A-D. The total number of deposited particles per  $\text{cm}^2$  (at 1.5 % deposition rate) along with their size distribution is reported in Fig. 9. The total number of deposited particles was 5.3 million in the Traffic, 1.9 million in the Urban, 1.7 million in the Industrial, and 0.33 million in the Background locality, respectively.

For the parameters in Figs. 6–8, we further calculated average daily values (Tables 2–Table 5). The data revealed that considerably higher levels of PM10/PM2.5 were detected in the Urban locality compared to other sampling sites. The sampling season may be responsible for this observation, as in the winter local heating significantly contributes to concentrations of ambient air pollutants. This observation is also in agreement with previous studies conducted in the Ostrava region.

Average daily particle number concentrations revealed that the Traffic locality was burdened by an extremely high number of particles, which several times exceeded the particle numbers in other localities. Size distribution analysis showed that the highest proportion of particles in this station was around 14.3 nm in size; the second peak was around 80 nm. In the Urban locality, a smaller peak at 50 nm was observed.

From other analyzed contaminants, we did not find any excessive concentrations of benzene, a VOC with a concentration limit of 5  $\mu\text{g}/\text{m}^3$ . Its values were lower in the Industrial locality than in the Urban station. In contrast, BaP concentrations in the Urban locality were several-fold higher than the limit of 1 ng/ $\text{m}^3$ . Finally, in the Traffic locality, average NOx concentrations exceeded more than two-fold the concentration limit of 30  $\mu\text{g}/\text{m}^3$ . However, it should be highlighted that the concentration limits are set for yearly averages, while our measurements were based on 5-day observations. Concentrations of other organic compounds determined in the Industrial and Urban localities are shown in Supplementary File S3 and Supplementary File S4.

Meteorological conditions varied throughout the field campaigns (Tables 2–5). There was a significant amount of precipitation during the experiments in the Background locality, while in the Industrial and Traffic localities the weather was mostly dry, with rather high temperatures. The campaign in the Urban locality was performed in the winter season, with light snow/snow accumulation and low temperatures

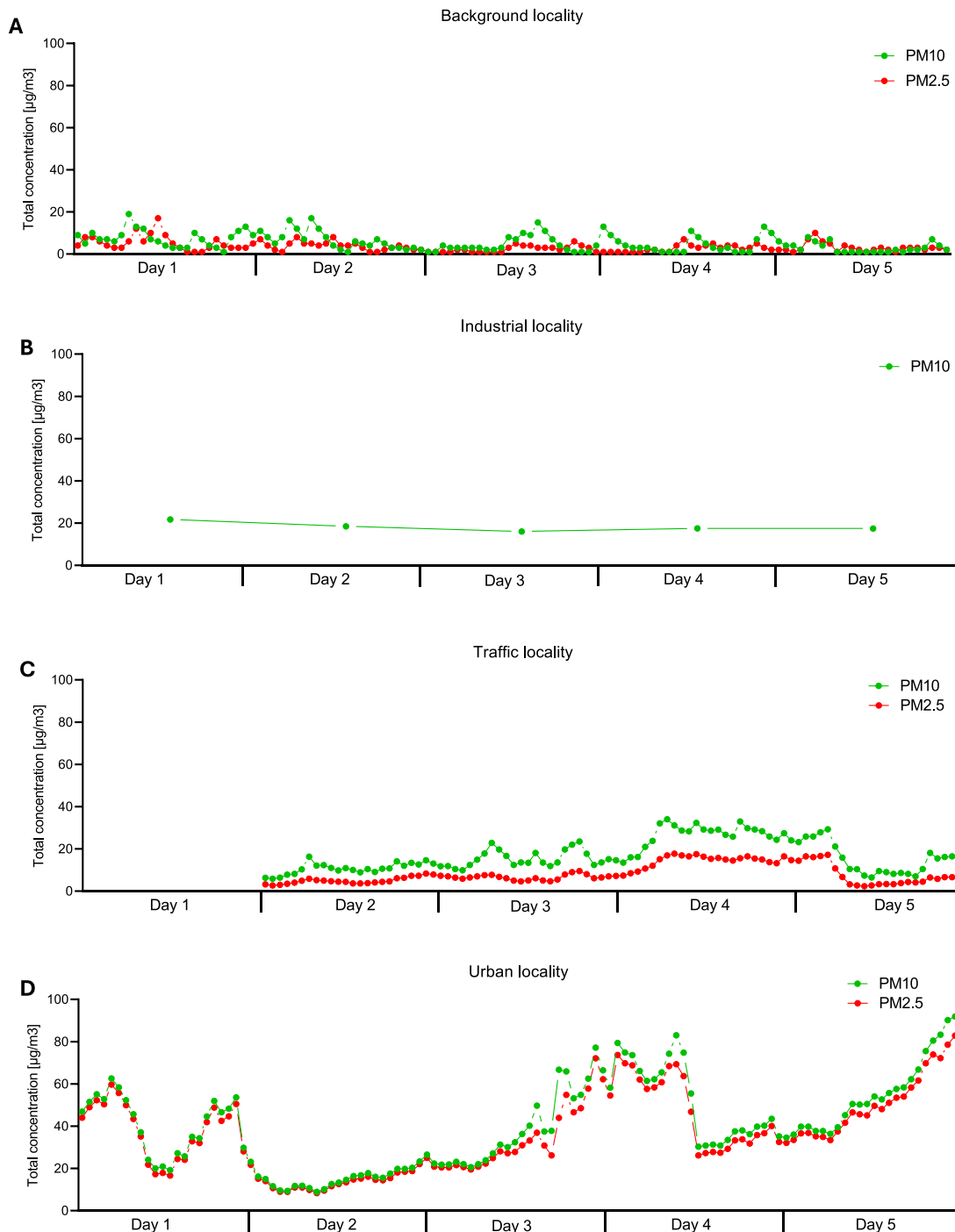


**Fig. 6.** Hourly distribution of mass concentration of PM10 and PM2.5 over the five-day exposure period (Day 1-Day 5) in A) Background, B) Industrial, C) Traffic and D) Urban localities. Due to technical reasons, for the Industrial locality only average daily PM10 concentrations are available.

(below 0 °C).

### 3.2. Biological analyses

#### 3.2.1. TEER measurement

TEER measurement is an important indicator of tissue integrity. The TEER values for each sample were measured at two-time intervals, before exposure (T0) and after five-day exposure (T5) to ambient air in tested localities/control air. As illustrated in Fig. 10, the TEER level of MucilAir™ tissue from asthmatic subjects was generally slightly lower than the respective tissue from healthy donors within each locality and time interval (with the exception of asthma tissue exposed in the

Industrial locality at T5 versus healthy tissue at the same time interval). The difference was, however, not significant in either case. The TEER level of both asthmatic and healthy tissues exposed in the Traffic locality at T5 was deeply below the minimal acceptable value (200 Ω.cm<sup>2</sup>) indicating poor condition of cells at this time interval. A significant difference was found between MucilAir™ asthma tissue exposed in this locality at T5 versus asthma tissue from the Industrial locality at T5 and T0. We further observed a significant difference in TEER level of MucilAir™ healthy tissue exposed in the Traffic locality at T5 versus MucilAir™ healthy tissues exposed in other localities at T5 (Background, Industrial, Urban), the control healthy tissue as well as healthy tissue exposed in the Traffic locality at time interval T0. Due to cell death

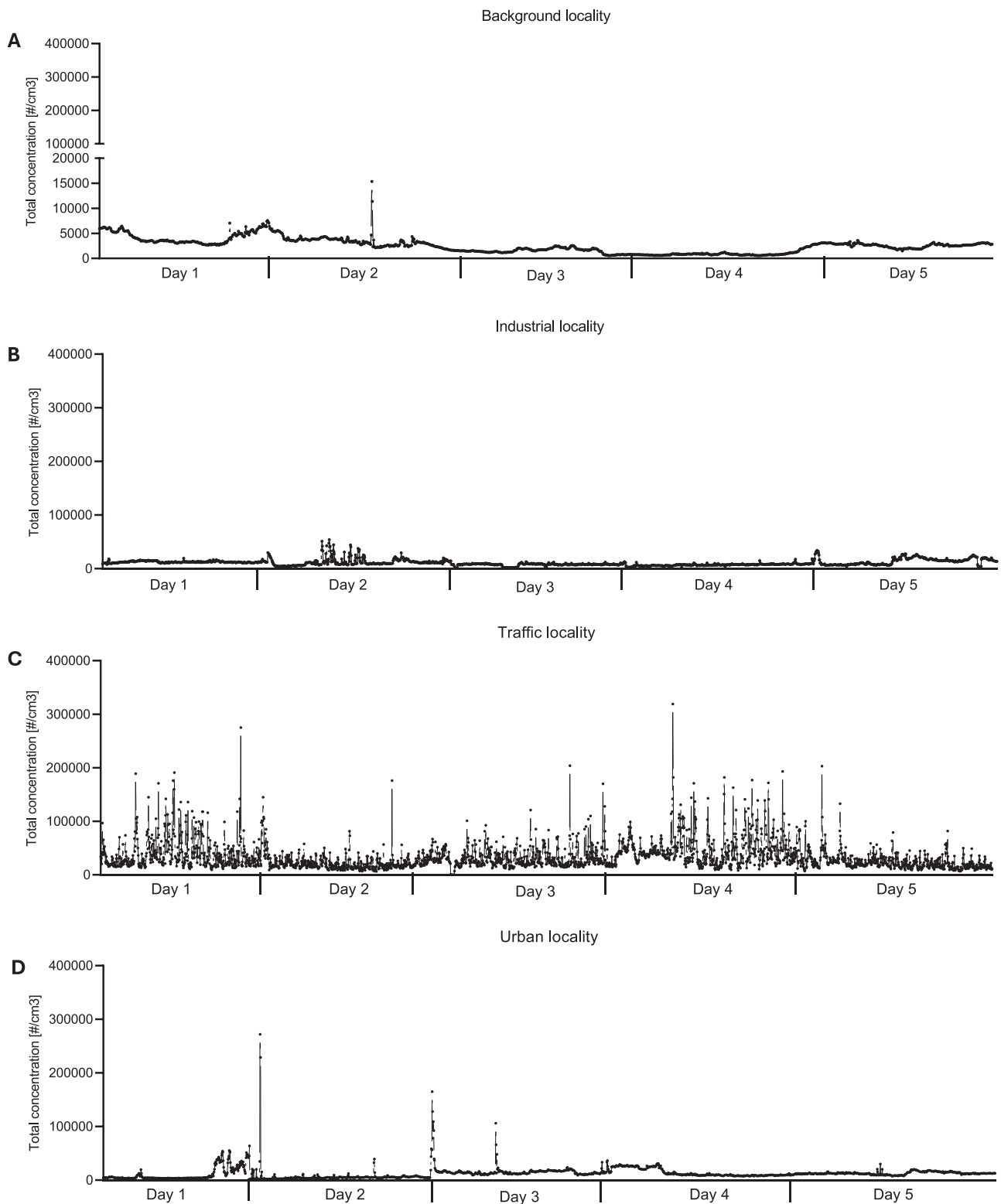


**Fig. 7.** Particle number distribution over the five-day exposure period in A) Background, B) Industrial, C) Traffic and D) Urban localities.

after the five-day exposure, no other parameters [except for adenylate kinase (AK) levels, a marker of cytotoxicity] were measured in tissues exposed in the Traffic locality.

### 3.2.2. Cytotoxicity

The release of intracellular enzymes lactate dehydrogenase (LDH) and AK are associated with cell lysis upon damage and are used as

markers of cytotoxicity. Relative LDH and AK activities were measured in the exposed and control MucilAir™ tissues after five-day exposure (T5) to ambient air in the cell culture medium. In the Traffic locality, the AK levels were analyzed in most of time intervals (T0 – T3, T5). The LDH relative activity was around 30 % in both asthmatic and healthy MucilAir™ control tissues and also in both MucilAir™ tissues exposed in Background, Industrial and Urban localities (Fig. 11A). Relative AK

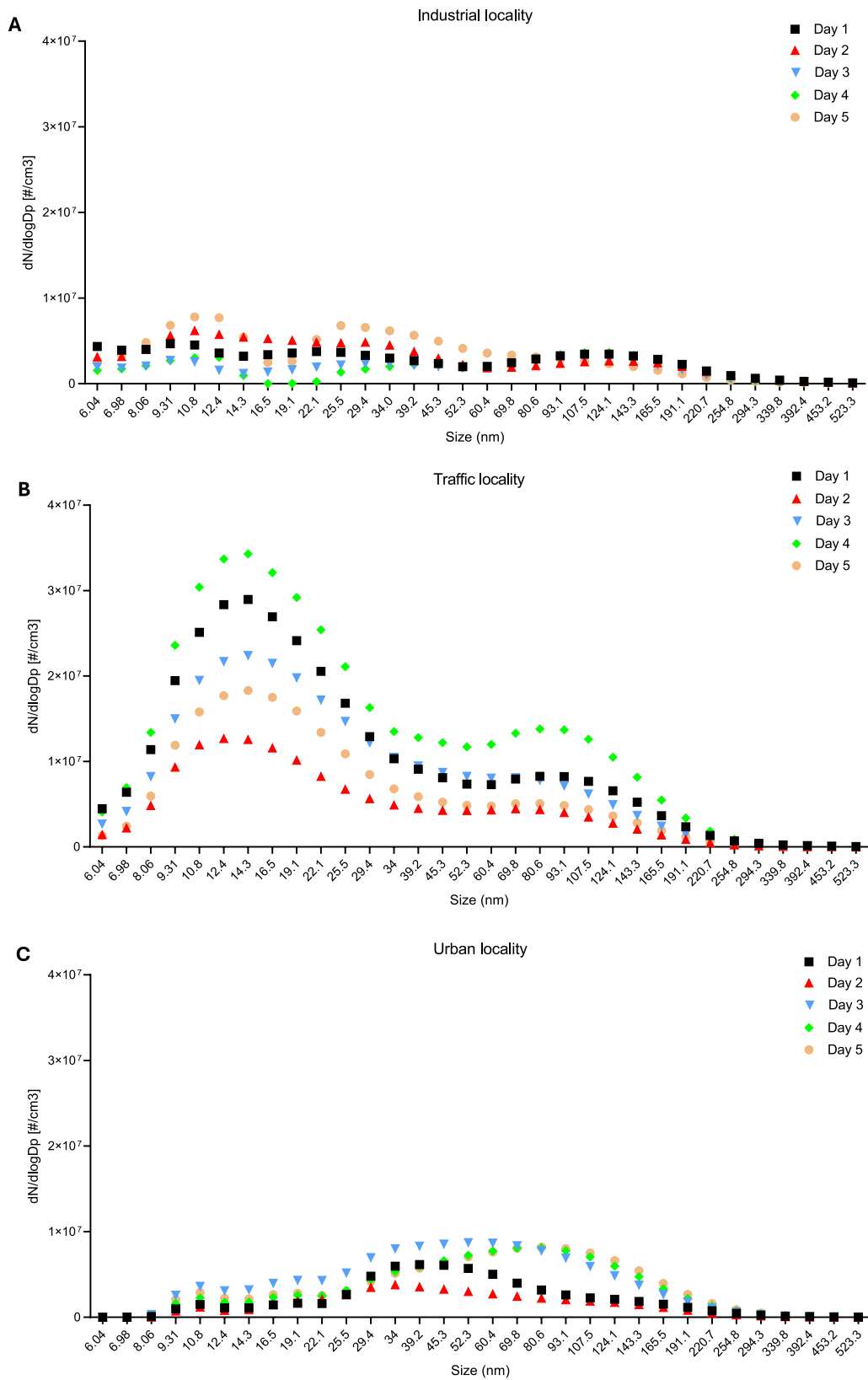


Fig. 8. Size distribution of particles over the five-day exposure period in A) Industrial, B) Traffic and C) Urban localities.

levels in MucilAir™ from healthy tissues exposed to polluted air in the Urban locality were significantly lower than those of MucilAir™ from asthmatic samples exposed in the same city and also lower than control MucilAir™ from healthy tissues. The highest median AK levels did not

exceed 5% except for the MucilAir™ asthma sample exposed in the Urban locality that reached 6.12% (Fig. 11B). In the Traffic locality, AK levels have reached high values, mostly exceeding 40%, in the first to third day of exposure (T1-T3; at T4, the sample was not collected). At T5,



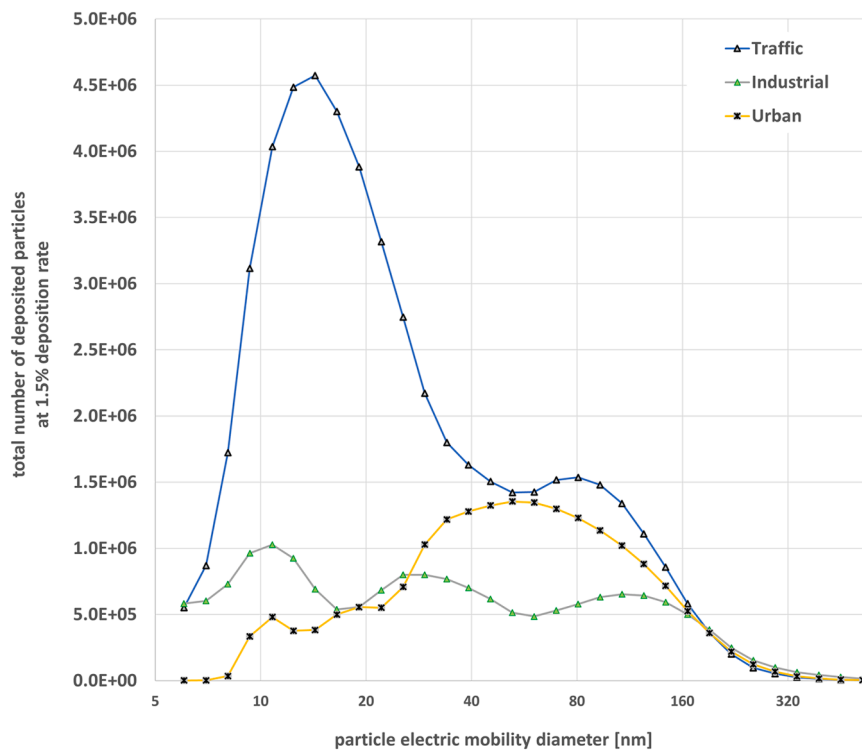


Fig. 9. The total number of deposited particles per cm<sup>2</sup> for individual particle size distributions over the exposure duration. At 2 exposures of 2 hours per day for five days, a flow rate of 25 cm<sup>3</sup>/min per insert, 6 mm insert diameter, and 1–2 % deposition efficiency by diffusion (the dominant mechanism as the number of larger particles was very small), the total deposited dose per cm<sup>2</sup> was 0.33 million in the Background, 1.7 million in the Industrial, 1.9 million in the Urban and 5.3 million in the Traffic locality, respectively. No particle size distribution is given for the Background locality due to low particle concentrations.

Table 2

Mean daily concentrations of relevant ambient air contaminants and meteorological conditions in the Background locality (yearly exposure limits for relevant parameters in parentheses).

Kosetice-Background	Sampling date					Mean
	4.8.2023	5.8.2023	6.8.2023	7.8.2023	8.8.2023	
PM10 (µg/m <sup>3</sup> ) (exp. limit 40 µg/m <sup>3</sup> )	7.5	6.7	4.5	4.7	3.0	5.3
PM2.5 (µg/m <sup>3</sup> ) (exp. limit 20 µg/m <sup>3</sup> )	5.4	3.9	2.4	2.7	3.0	3.5
Particle number conc. (#/cm <sup>3</sup> )	4319	3258	1507	924	2620	2526
Min. temperature (°C)	15.2	13.7	12.9	10.7	9.9	14.7
Max. temperature (°C)	22.6	18.2	16.9	14.7	19.4	18.4
Mean temperature (°C)	18.8	14.2	13.8	12.2	14.7	12.5
Mean air humidity (%)	61	95	88	85	68	79.4
Precipitations (mm)	8.0	30.3	9.7	6.5	2.6	11.4
Sunshine (h)	2.0	0.0	0.3	0.6	3.9	1.4
Mean wind speed (m/s)	2.3	5.3	5.6	7.3	4.5	5.0

Table 3

Mean daily concentrations of relevant ambient air contaminants and meteorological conditions in the Industrial locality (yearly exposure limits for relevant parameters in parentheses).

Kvasiny-Industrial	Sampling date					Mean
	21.8.2023	22.8.2023	23.8.2023	24.8.2023	25.8.2023	
PM10 (µg/m <sup>3</sup> ) (exp. limit 40 µg/m <sup>3</sup> )	21.7	18.5	16	17.5	17.4	18.2
Particle number conc. (#/cm <sup>3</sup> )	12496	12557	7400	7353	14083	10778
Benzene (µg/m <sup>3</sup> ) (exp. limit 5 µg/m <sup>3</sup> )	0.20	0.20	0.20	0.10	0.10	0.16
Min. temperature (°C)	20.1	18.8	17.3	16.5	18	18.1
Max. temperature (°C)	28	28.3	23.8	25.4	25.9	26.3
Mean temperature (°C)	22.2	23.2	19.3	20.7	21.3	21.3
Mean air humidity (%)	78	66	67	61	74	69.2
Precipitations (mm)	0	0	0	0.1	0.4	0.1
Sunshine (h)	7.3	9.3	9.8	10.8	8.9	9.2
Mean wind speed (m/s)	2.4	2.1	2.2	1.3	2.2	2.0

**Table 4**

Mean daily concentrations of relevant ambient air contaminants and meteorological conditions in the Traffic locality (yearly exposure limits for relevant parameters in parentheses).

Prague-Traffic	Sampling date					Mean
	18.9.2023	19.9.2023	20.9.2023	21.9.2023	22.9.2023	
PM10 ( $\mu\text{g}/\text{m}^3$ ) (exp. limit 40 $\mu\text{g}/\text{m}^3$ )		10.7	15.4	26.2	15.4	16.9
PM2.5 ( $\mu\text{g}/\text{m}^3$ ) (exp. limit 20 $\mu\text{g}/\text{m}^3$ )		4.9	6.6	14.1	7.6	8.3
Particle number conc. ( $\#/ \text{cm}^3$ )	42166	20536	30949	48295	23737	33137
NOx ( $\mu\text{g}/\text{m}^3$ ) (exp. limit 30 $\mu\text{g}/\text{m}^3$ )		46.39	83.48	133.94	61.31	81.28
Min. temperature ( $^{\circ}\text{C}$ )	13.7	14.9	11.8	12.5	12.9	13.2
Max. temperature ( $^{\circ}\text{C}$ )	28.7	23.7	25.5	23.6	18.7	24.0
Mean temperature ( $^{\circ}\text{C}$ )	19.9	17.8	18.6	18.1	15	17.9
Mean air humidity (%)	73	62	63	77	82	71.4
Precipitations (mm)	0.9	0	0	0	4.8	1.1
Sunshine (h)	8.9	5.3	11.1	6.8	0.1	6.4
Mean wind speed (m/s)	2.5	5.2	3.2	2.7	3.6	3.4

**Table 5**

Mean daily concentrations of relevant ambient air contaminants and meteorological conditions in the Urban locality (yearly exposure limits for relevant parameters in parentheses).

Ostrava-Urban	Sampling date					Mean
	2.12.2023	3.12.2023	4.12.2023	5.12.2023	6.12.2023	
PM10 ( $\mu\text{g}/\text{m}^3$ ) (exp. limit 40 $\mu\text{g}/\text{m}^3$ )	41.0	15.1	37.8	53.6	54.5	40.4
PM2.5 ( $\mu\text{g}/\text{m}^3$ ) (exp. limit 20 $\mu\text{g}/\text{m}^3$ )	38.4	13.9	32.6	48.6	49.8	36.6
Particle number conc. ( $\#/ \text{cm}^3$ )	10736	6103	16344	14073	12800	12011
Benzene ( $\mu\text{g}/\text{m}^3$ ) (exp. limit 5 $\mu\text{g}/\text{m}^3$ )	3.90	2.90	3.60	4.70	4.00	3.82
BaP ( $\text{ng}/\text{m}^3$ ) (exp. limit 1 $\mu\text{g}/\text{m}^3$ )	6.20	1.00	5.50	5.80	8.00	5.30
Min. temperature ( $^{\circ}\text{C}$ )	-2.8	-6.6	-6.5	-8.6	-1.9	-5.3
Max. temperature ( $^{\circ}\text{C}$ )	-0.3	-1.5	-0.2	1.1	0.9	0.0
Mean temperature ( $^{\circ}\text{C}$ )	-2.5	-4.5	-3.2	-1.8	-0.2	-2.4
Mean air humidity (%)	94	86	77	82	91	86.0
Precipitations (mm)	10.6	3.4	0	0	2.4	3.3
Sunshine (h)	0	1.6	5.6	3.2	0	2.1
Mean wind speed (m/s)	3.2	1.2	0.9	1.4	1.3	1.6

the levels sharply dropped, probably reflecting cell death at this time interval (Supplementary Figure 6).

### 3.2.3. 15-F<sub>2t</sub>-isoprostane

IsoP is a product of lipid peroxidation, therefore, it was used to evaluate and characterize the potential oxidative damage following five-day exposure. However, no significant changes in IsoP levels were observed in any locality indicating no impacts of our experimental settings on the levels of peroxidized lipids (Fig. 12).

### 3.2.4. Cytokines, chemokines and growth factors

The production of selected immune response-related molecules was analyzed following the five-day exposure. The set of inflammatory markers consisted of 20 molecules, including cytokines (TNF $\alpha$ , IL-6, IL-7, IL-1 $\alpha$ , IL-1 $\beta$  and IL-1RA) chemokines (Eotaxin, GRO $\alpha$ , IP-10, MCP-1, MIP-1 $\alpha$ , MIP-1 $\beta$ , RANTES, SDF-1 $\alpha$ ) and growth factors (BDNF, EGF, GM-CSF, LIF, PIGF-1, VEGF-A). Overall, we observed the most pronounced differences between samples exposed in the Urban and Industrial localities. For this comparison, a significantly higher production of Eotaxin, GM-CSF, GRO $\alpha$ , MIP-1 $\alpha$  and TNF $\alpha$  in both the asthmatic and healthy tissues exposed in the Industrial locality was found; GRO $\alpha$  production was not detected in the Background station. The level of IL-6 and IL-7 was specifically elevated only in the asthmatic tissue exposed in the Industrial locality when compared with the Urban locality while an increase of SDF-1 concentrations was observed only for the healthy tissue for this comparison. IL-1b production was elevated in asthmatic tissues exposed in the Background station than those in the Urban station. The same cytokine was not detected in any of these tissues exposed in the Industrial locality. IP-10 was not detected in either Urban sample (Fig. 13).

## 4. Discussion

Investigating the mechanisms of the biological effects of ambient air pollution is a challenging task for which researchers have not yet found a satisfactory solution. Due to the complexity of the human organism, conclusive information can only be obtained in population studies. However, such projects are limited by their costs and logistics, as well as by ethical considerations. Therefore, in toxicology, various cell models and exposure scenarios have been introduced (Faber and McCullough, 2018). Over the years it has become apparent that experiments in strictly laboratory settings (i.e., a single cell line, commonly of a tumor origin; unrealistic testing doses; chemicals applied individually, rather than in mixtures) are too artificial to generate data that can be extrapolated to real-world human exposure. For inhalation toxicology, finding the optimal mode of application of air pollutants is one of the greatest obstacles. This fact stems from the presence of mixtures of contaminants differing in chemical composition and state (a combination of solid, gaseous and liquid components). The introduction of the ALI systems was a step in the right direction, as they have the potential to deliver mixtures of air pollutants to the cells in a form that better resembles the real tissue/organ (Aufderheide, 2005). However, due to their technical construction, these systems are usually restricted to being used in laboratory settings, with a very limited option of mobility. Therefore, they cannot satisfy the need to monitor the biological impacts of air pollutants in field conditions.

In our study, we have built upon our previously constructed exposure box (Vojtisek-Lom et al., 2019), combined it with a modified commercial cell incubator, added other laboratory and technical equipment (a flow box, a freezer, another cell incubator, CO<sub>2</sub> flasks, energy source, systems to monitor air pollutants as needed for the experiment) and

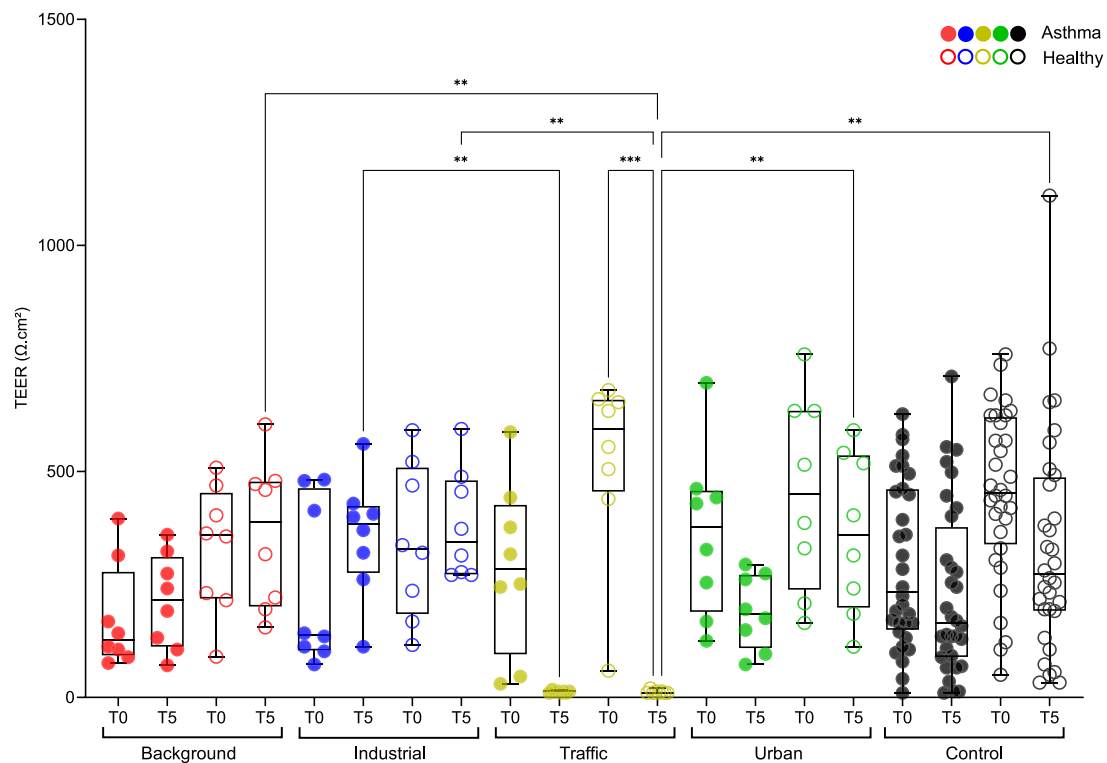


**Fig. 10.** Transepithelial electric resistance measurement following the exposure of MucilAir tissues to ambient air in distinct localities (Background, Industrial, Traffic, Urban) or control air (Control) at two-time intervals, T0 and T5. Tissues were reconstituted from asthmatic (filled circles) or healthy (empty circles) donors. Asterisks denote significant difference between indicated pairs (\* $p < 0.05$ , \*\* $p < 0.01$ , \*\*\* $p < 0.001$ , Kruskal-Wallis test).

transported it in a van to diverse localities of the Czech Republic. We proved that such a setting satisfies the required aims and that the lung tissue models respond to the ambient air in diverse ways, reflecting differences in air pollution and/or meteorological conditions, as well as disease (asthma)/health status.

Despite an improvement in air quality in developed countries, air pollution still remains a significant factor responsible for increased morbidity and excess mortality. It is estimated that in 2019, 74 % of total deaths resulted from non-communicable diseases, of which 20 % can be attributed to environmental factors. Among them, ambient air pollution is estimated to be responsible for 50 % of the deaths (Poizzer et al., 2023). Negative health impacts are manifested even at very low ambient concentrations of PM<sub>2.5</sub>, if the exposure lasts long enough. Importantly, excess mortality from ambient air pollution has increased over the last decade (Poizzer et al., 2023). All these facts implicate the importance of further research in the field of the biological impacts of environmental air pollutant exposure.

Our study was intended as a step in this direction, aiming to develop an innovative system for the field monitoring of ambient air pollution-related molecular changes in a relevant lung tissue model. To the best of our knowledge, only three attempts have been made to monitor ambient air pollution using an ALI system. In 2015, Vizuet et al. reported the development of a system allowing the measurement of gene expression changes in human lung cells upon direct exposure in the field (Vizuet et al., 2015). They exposed the human epithelial lung A549 cell line to air pollution sources from the Houston Ship Channel for three days and observed changes in expression of genes related to immune response and inflammation. Although measurements in the field were performed, the system was not designed to be mobile thus limiting its deployment to any location. It should also be noted that the cell model was of tumor origin, which may have negatively impacted the data interpretation, particularly if this was based on gene expression analyses.

In a study published in 2018, Bisig et al. exposed a multicellular lung

model to ambient air in Fribourg, Switzerland (Bisig et al., 2018). The 3-day exposures were conducted in summer and winter in the same locality. In the winter samples, increased expression of pro-inflammatory genes was noted reflecting higher concentrations of air pollutants in this season. Although the system was declared as mobile, the authors did not show any attempt to deploy it to different localities and demonstrate the feasibility of its relatively easy transportation nor publish follow-up studies as planned in the conclusions of the article.

In 2018, Gualtieri et al. reported the application of a system allowing direct exposure of BEAS-2B cells cultured at ALI to environmental concentrations of particulate matter (Gualtieri et al., 2018). In this and follow-up studies by the same group (Costabile et al., 2023; Santoro et al., 2024) the authors investigated the expression of immune response, oxidative stress and xenobiotic metabolism-related genes, as well as DNA methylation in promotor regions of selected genes. Interestingly, while impacts of PM on gene expression were detected, DNA methylation in was not affected suggesting the involvement of other epigenetic mechanisms in the gene deregulation.

Our system is unique in its ability to be freely transported to any location and optionally be operated even without direct access to electrical power (provided that a battery of sufficient capacity is used). This was demonstrated by the system deployment at four diverse localities of the Czech Republic. We designed our experiments so that they represent various types of environment and sampling seasons. As we did not aim to directly compare effects of different concentrations of air pollutants and impacts of meteorological conditions, our experiments were conducted during the entire year in localities with diverse sources of ambient air toxicants. Overall, the biological changes that we observed are relatively weak: apart from the Traffic locality, where the air pollutants caused the early death of cell cultures, we did not find any major differences in TEER, cytotoxicity and lipid peroxidation in relation to the exposure of ambient air. These results were unexpected as there were potentially significant variables that may have impacted overall biological impacts of ambient air exposure, particularly the sampling season (winter

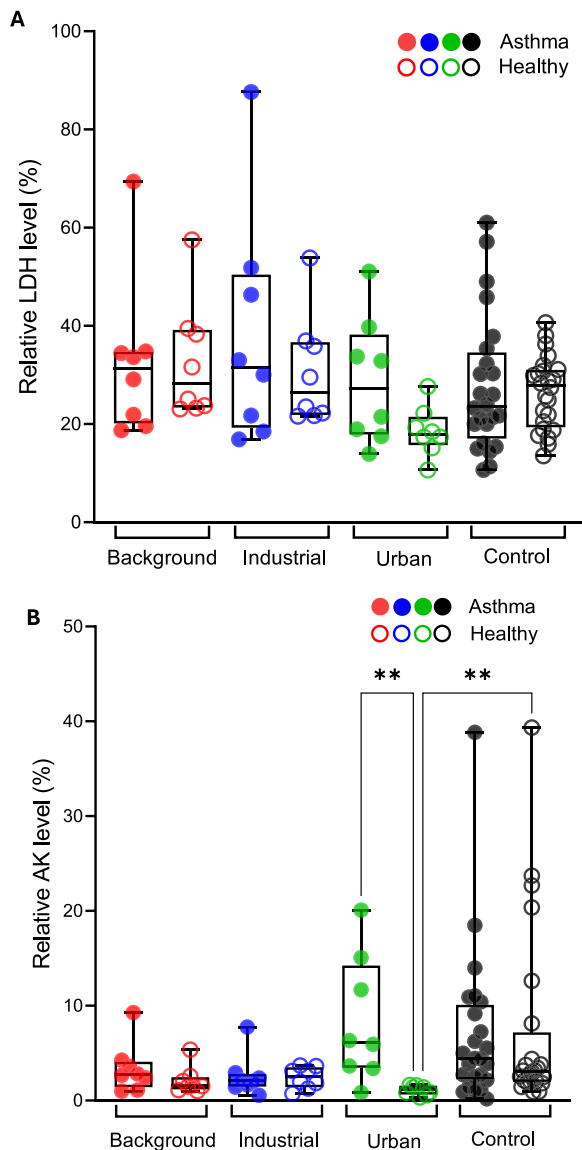


**Fig. 11.** Cytotoxic response following the five-day exposure of MucilAir™ tissues to ambient air in distinct localities (Background, Industrial, Urban) or control air (Control). Cytotoxicity was analyzed by measuring the relative levels of A) lactate dehydrogenase and B) adenylate kinase released from the exposed or control tissues into the basolateral medium. Tissues were reconstituted from asthmatic (filled circles) or healthy (empty circles) donors. Asterisks denote significant difference between indicated pairs (\* $p < 0.05$ , \*\* $p < 0.01$ , \*\*\* $p < 0.001$ , Kruskal-Wallis test).

months are characterized by increased concentrations of pollutants due to local heating and/or atmospheric inversions).

Although ambient air pollutants are present in a complex mixture of many compounds, particulate matter, especially that of a small aerodynamic diameter, is a key component driving the primary biological response of the target organism. PM is mostly responsible for the induction of oxidative stress (Daiber et al., 2020), a relatively non-specific response that is, however, linked with a number of biological changes in the organism (Klaunig, 2018). Therefore, we specifically focused on particles characterization by assessing their number concentration and size distribution (using our monitoring systems), as well as PM<sub>2.5</sub> and PM<sub>10</sub> concentrations (using the equipment/data of the CHMI, where available). As expected, in the Background locality the PM contamination was very low. In contrast, in the Urban locality PM<sub>2.5</sub> and PM<sub>10</sub> concentrations were the highest, even exceeding recommended

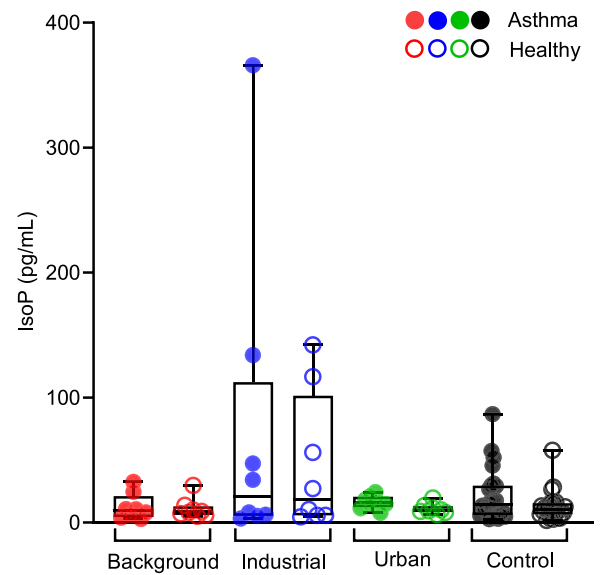


**Fig. 12.** The level of IsoP determined in MucilAir™ tissues after the five-day exposure to ambient air in distinct localities (Background, Industrial, Urban) or control air (Control). Tissues were reconstituted from asthmatic (filled circles) or healthy (empty circles) donors. Asterisks denote significant difference between indicated pairs (\* $p < 0.05$ , \*\* $p < 0.01$ , \*\*\* $p < 0.001$ , Kruskal-Wallis test).

exposure limits. This result confirmed the data of the long-term air pollution monitoring in this locality identifying it a hotspot of ambient air pollutants in the Czech Republic (Rossner et al., 2013). In agreement with PM levels, the concentrations of BaP were also high. Interestingly, differences in PM concentrations were not reflected in the biological parameters assessed in our study. We believe that the exposure time was too short for the effects to be manifested.

In the Traffic locality we unexpectedly were not able to perform our analyses at the T5 time point, as the cell cultures were not viable at this exposure interval. The analysis of particle characteristics revealed an exceptionally high total number concentration, as well as ultrafine particles concentration (peaks at around 14 nm and 100 nm) when compared with other localities. In addition, NO<sub>x</sub> concentrations more than two-fold exceeded the exposure limits for this pollutant. As previously shown, traffic is a major source of ambient air ultrafine particles and NO<sub>x</sub> (Wahlina et al., 2001). Thus, our exposure system reflected the high environmental burden caused by heavy traffic. This was confirmed by the analyses of cytotoxicity, that was significantly elevated in the exposed samples already in the first day of the experiment. Follow-up studies with shorter exposure intervals will allow us to identify the mechanisms of the biological response of the MucilAir™ model affected by high concentrations of traffic-related pollutants.

The residents of the Industrial locality have complained of subjectively poor ambient air quality, commonly reporting a smell of unknown origin and smoke of various colors emitted by the wood-processing plant. The measurements have been repeatedly conducted by factory owners and state authorities, however, none of the analyzed pollutants exceeded exposure limits. We thus intended to use our exposure system to identify possible biological changes in the tissue model, given that no alterations in the chemical composition of the ambient air were detected. In addition, we performed a comprehensive chemical analysis of the ambient air, specifically focusing on the compounds contained in the paint (e.g., VOCs and other organics), but did not find any excessive values in those common pollutants that were analyzed; this does not rule out the possible presence of other problematic compounds, especially these that may be objectionable or harmful at relatively very low concentrations.

The biological tests, however, showed differences in some immune

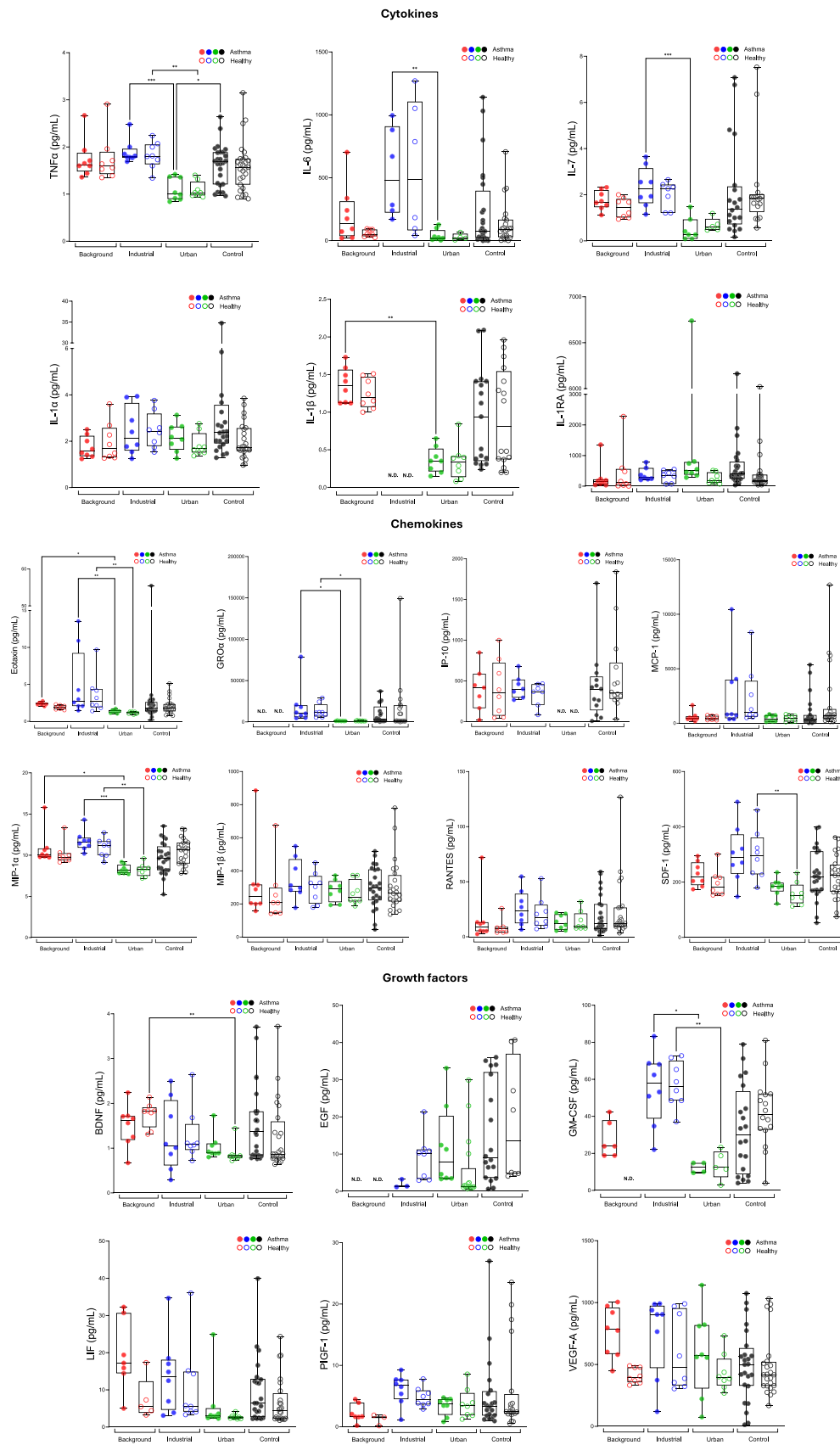


**Fig. 13.** Production of immune response-relevant molecules by MucilAir™ tissues after the five-day exposure to ambient air in distinct localities (Background, Industrial, Urban) or control air (Control). Tissues were reconstituted from asthmatic (filled circles) or healthy (empty circles) donors. Asterisks denote significant difference between indicated pairs (\* $p < 0.05$ , \*\* $p < 0.01$ , \*\*\* $p < 0.001$ , Kruskal-Wallis test).

response-related molecules (TNF $\alpha$ , MIP-1 $\alpha$ , Eotaxin, GRO $\alpha$  and GM-CSF for both types of samples; IL-6, IL-7 for asthmatic only; SDF-1 for healthy only) when compared with the Urban locality.

The multifunctional cytokine TNF $\alpha$  is produced by a variety of cells and acts as an important mediator in many cytokine-dependent inflammatory events. Due to its pro-inflammatory and pro-oxidant properties, TNF $\alpha$  represents a complication for many diseases: it plays a significant role in pulmonary pathophysiology, has been implicated in asthma, chronic bronchitis, COPD, acute lung injury and acute respiratory distress syndrome (Mukhopadhyay et al., 2006). The secretion of TNF $\alpha$  in lungs in response to the exposure to airborne PM or diesel exhaust particles has been evidenced by several studies (Camarinho et al., 2019; Kumar et al., 2017; Tsai et al., 2012; van Eeden et al., 2001).

MIP-1 $\alpha$  (CCL3) is a pro-inflammatory chemokine produced by lymphocytes, resident and recruited monocytes and macrophages, fibroblasts, and epithelial cells during infection or inflammation. It exerts chemotactic activities toward a variety of immune cells thus mediating inflammation and participates in many pulmonary diseases. A recent study (Roffel et al., 2020) suggested the possible role of CCL3 as an important mediator in asthma and COPD due to its function as a chemoattractant for monocytes/macrophages and neutrophils. Several studies have investigated the role of CCL3 in respiratory allergies. Grass pollen, ragweed or birch and oak dusts have been shown to increase CCL3 levels *in vivo* and *in vitro* (Erin et al., 2005; Kostova et al., 2015; Määttä et al., 2005).

Eotaxin (CCL11) is crucial in eosinophil chemoattraction and activation in the pathogenesis of asthma and has also been associated with COPD (George and Brightling, 2016). It may also enhance lung fibrosis (Puxeddu et al., 2006) and lung cancer (Lin et al., 2021). Upregulated expression of *CCL11* was observed in human lung cells following exposure to diesel exhaust particles (Takizawa et al., 2003) or complete ambient air 12.

GRO $\alpha$  (CXCL1) acts as a chemoattractant for neutrophils, an important component of the immune defense barrier. These cells are one of the first cells recruited to the site of infection thus playing a crucial role in several pulmonary diseases (Arora and Singh, 2024). GRO $\alpha$  activity has been associated with asthma, COPD, chronic rhinosinusitis and infectious respiratory diseases (Korbecki et al., 2022). In accordance with our study, upregulated expression of *CXCL1* was observed in lung alveolar macrophages following exposure to diesel exhaust particles (Salvi et al., 2000) and in lung bronchial epithelial cells following exposure to PM<sub>2.5</sub> (Zhou et al., 2015).

GM-CSF is a major regulator of inflammatory cells of the myeloid lineage. Besides this function it also has several biological activities on eosinophils, the predominant cells in bronchial asthma and plays a key role in many autoimmune and inflammatory diseases. GM-CSF has been implicated in lung bacterial, fungal, and viral infections, interstitial lung disease, allergic lung disease, alcoholic lung, and other disease states (Chen et al., 2023). It was demonstrated that particulate pollutants such as ambient particulate matter or diesel exhaust particles stimulate production of GM-CSF in human lung cells (Boland et al., 2000; Reibman et al., 2002).

Air pollution is known to be associated with the increased incidence of asthma and also with the worsening of the symptoms of current asthma. We observed that IL-6 and IL-7 levels were significantly increased specifically in asthma tissue exposed in the Industrial locality compared to the asthma tissue exposed in the Urban site. IL-6 is a pleiotropic cytokine that influences inflammatory reactions such as acute phase protein generation, inflammation or antigen-specific immune responses. It is also involved in many physiological processes such as hematopoiesis, apoptosis, differentiation, and cellular metabolism (Uciechowski and Dempke, 2020). As evidenced by numerous studies, IL-6 signaling plays a critical role in the development of asthma. Elevated IL-6 levels have been found in the serum, induced sputum and bronchoalveolar lavage fluid (BALF) of asthmatic patients, and have been linked to impaired lung function and asthma severity (Chen et al.,

2022). Despite the fact, that increased IL-6 is implicated in other inflammatory diseases, its role in asthma diagnosis is undisputable and has been acknowledged as a biomarker of asthma severity (Pan et al., 2023; Peters et al., 2020).

The role of IL-7 in asthma is not fully elucidated. However, it was demonstrated that IL-7 increases the production of eosinophils (Chen et al., 2021). Accumulation of these cells in airways defines an asthma subtype called eosinophilic asthma. Eosinophils play a critical role in asthma diagnosis, and it has been reported that eosinophils are important predictors of disease severity and progression (Hussain and Liu, 2024).

SDF-1 (CXCL12) was the only chemokine specifically elevated in healthy tissue exposed in Industrial versus Urban locality. This chemokine is secreted mainly by pulmonary fibroblasts and together with its receptor CXCR4 it participates in multiple pathological mechanisms of fibrosis such as inflammation, epithelial-mesenchymal transition, and angiogenesis (Wu et al., 2023). It has been demonstrated that CXCL12/CXCR4 axis is a potential shared mechanism for diverse types of pulmonary fibrosis which can occur in a number of lung disorders such as idiopathic pulmonary fibrosis (IPF), pneumoconiosis, COPD, and coronavirus disease (Qi et al., 2024).

Overall, our data show that exposure of asthmatic and healthy MucilAir™ tissues to complete ambient air in the Industrial locality resulted in the modulation of selected immune response-related molecules. This may potentially lead to the development of various respiratory diseases or exacerbation of existing diseases such as asthma, COPD, pulmonary fibrosis and many others. Biologically, these observations are very important; however, the question of which factors were responsible for such differences remains. The levels of air pollutants that were monitored in our study and possess pro-inflammatory properties (PM, BaP, benzene) were higher in the Urban locality. This would imply that cytokine/chemokine levels should be increased in the samples exposed in this locality when compared with the Industrial one. The opposite results that we obtained can be explained by the sampling period (winter vs. summer) and ambient air contaminants related to the growing season. Some plant-related products, particularly pollen grains, are strongly immunogenic and have been shown to induce cytokine production (Cecchi et al., 2022; Gilles et al., 2012). The effects may even be potentiated by the presence of environmental pollutants, such as diesel exhaust (Candeias et al., 2022). Our data thus indicate that the expression immune response-related molecules can be elevated in an environment where concentrations of industrial/traffic pollutants do not exceed recommended exposure limits. This also corresponds to the fact that we did not observe a significant difference in the immune response-related molecules between the Industrial and Background localities which had the lowest level of air pollutants. Finally, we can also speculate that other chemical compounds that we did not monitor were present in the ambient air of the Industrial locality resulting in elevated production of these molecules. For this hypothesis, however, we do not have any experimental data.

## 5. Study limitations

Despite being carefully planned and performed, the study has some potential limitations that need to be acknowledged. (1) The study design does not allow to distinguish between the effects of particles and other ambient air pollutants (e.g., volatile compounds). However, the primary aim of our investigation, to prove the feasibility of a mobile exposure system deployed at diverse locations at various environmental conditions, was achieved. (2) Although several classes of ambient air pollutants were monitored, only characteristics of particulate matter were commonly assessed in all studied localities. This approach was mainly driven by the relevance of individual types of pollutants in the localities. As PM, especially that of a small size (ultrafine particles), represents a significant health risk, we believe that our results still bring valuable information on biological impacts of air pollution. (3) The samples that

we exposed to ambient air originated from human volunteers of both genders, that might affect the results, as we did not include sex as a confounding factor in our analyses. This is also true for potential effects of genetic polymorphisms in relevant genes. However, our sample size was too small to account for these parameters. It should be mentioned that we intentionally designed the study to include diverse samples to mimic differences in real human population.

## 6. Conclusions

In our study, we demonstrated the feasibility of a mobile laboratory consisting of an exposure system, cell culture and air pollution measurement equipment and its application to assess the effects of ambient air pollutants on the lung tissue model grown at the air-liquid interface. Although the effects were generally weak, we proved the induction of immune response-related molecules, with a diverse response of the healthy and asthmatic tissues. We also showed traffic-related toxicity that significantly reduced the viability of the cell cultures. Our system proved to be an innovative approach for monitoring the biological response of environmental air pollution in a lung tissue model, with implications for health effects in human populations.

## CRedit authorship contribution statement

**Michal Vojtisek-Lom:** Writing – review & editing, Supervision, Project administration, Methodology, Investigation, Funding acquisition, Conceptualization. **Tereza Cervena:** Writing – review & editing, Methodology, Investigation. **Michal Sima:** Writing – review & editing, Visualization, Investigation, Formal analysis. **Zuzana Simova:** Writing – review & editing, Investigation. **Kristyna Vrbova:** Writing – review & editing, Investigation. **Michal Vojtisek:** Writing – review & editing, Investigation. **Martin Pechout:** Writing – review & editing, Investigation. **Helena Libalova:** Writing – review & editing, Writing – original draft, Visualization. **Lubos Dittrich:** Writing – review & editing, Methodology, Investigation. **Pavel Rossner:** Writing – review & editing, Writing – original draft, Supervision, Project administration, Funding acquisition, Conceptualization. **Antonin Ambroz:** Writing – review & editing, Investigation. **Zuzana Novakova:** Writing – review & editing, Investigation. **Fatima Elzeinova:** Writing – review & editing, Investigation. **Anezka Vimrova:** Writing – review & editing, Visualization, Investigation.

## Declaration of Competing Interest

The authors declare that they have no known competing financial interests or personal relationships that could have appeared to influence the work reported in this paper.

## Acknowledgements

Supported by the Czech Science Foundation (22-10279S). The authors acknowledge the assistance provided by the Research Infrastructure NanoEnviCz, supported by the Ministry of Education, Youth and Sports of the Czech Republic under Project No. LM2023066 and the Research Infrastructure EATRIS-CZ, supported by the Ministry of Education, Youth and Sports of the Czech Republic under Project No. LM2023053.

## Appendix A. Supporting information

Supplementary data associated with this article can be found in the online version at [doi:10.1016/j.ecoenv.2024.117495](https://doi.org/10.1016/j.ecoenv.2024.117495).

## Data Availability

Data will be made available on request.

## References

- Arora, A., Singh, A., 2024. Exploring the role of neutrophils in infectious and noninfectious pulmonary disorders. *Int. Rev. Immunol.* 43, 41–61. <https://doi.org/10.1080/08830185.2023.2222769>.
- Aufderheide, M., 2005. Direct exposure methods for testing native atmospheres. *Exp. Toxicol. Pathol.* 57, 213–226. <https://doi.org/10.1016/j.etp.2005.05.019>.
- Bisig, C., Petri-Fink, A., Rothen-Rutishauser, B., 2018. A realistic in vitro exposure revealed seasonal differences in (pro-)inflammatory effects from ambient air in Fribourg, Switzerland. *Inhal. Toxicol.* 30, 40–48. <https://doi.org/10.1080/08958378.2018.1441926>.
- Boland, S., Bonvallot, V., Fournier, T., Baeza-Squiban, A., Aubier, M., Marano, F., 2000. Mechanisms of GM-CSF increase by diesel exhaust particles in human airway epithelial cells. *Am. J. Physiol. Lung Cell. Mol. Physiol.* 278, L25–L32. <https://doi.org/10.1152/ajplung.2000.278.1.L25>.
- Camarinho, R., Garcia, P.V., Choi, H., Rodrigues, A.S., 2019. Overproduction of TNF- $\alpha$  and lung structural remodelling due to chronic exposure to volcanogenic air pollution. *Chemosphere* 222, 227–234. <https://doi.org/10.1016/j.chemosphere.2019.01.138>.
- Candeias, J., Zimmermann, E.J., Bisig, C., Gawlitta, N., Oeder, S., Gröger, T., Zimmermann, R., Schmidt-Weber, C.B., Buters, J., 2022. The priming effect of diesel exhaust on native pollen exposure at the air-liquid interface. *Environ. Res.* 211, 112968. <https://doi.org/10.1016/j.envres.2022.112968>.
- Cecchi, L., Vaghi, A., Bini, F., Martini, M., Musarra, A., Bilò, M.B., 2022. From triggers to asthma: a narrative review on epithelium dysfunction. *Eur. Ann. Allergy Clin. Immunol.* 54, 247–257. <https://doi.org/10.23822/EurAnnACI.1764-1489.271>.
- Chen, S., Chen, Z., Deng, Y., Zha, S., Yu, L., Li, D., Liang, Z., Yang, K., Liu, S., Chen, R., 2022. Prevention of IL-6 signaling ameliorates toluene diisocyanate-induced steroid-resistant asthma. *Allergol. Int. Off. J. Jpn. Soc. Allergol.* 71, 73–82. <https://doi.org/10.1016/j.alit.2021.07.004>.
- Chen, Y., Li, F., Hua, M., Liang, M., Song, C., 2023. Role of GM-CSF in lung balance and disease. *Front. Immunol.* 14, 1158859. <https://doi.org/10.3389/fimmu.2023.1158859>.
- Chen, Y., Luo, X.-S., Zhao, Z., Chen, Q., Wu, D., Sun, X., Wu, L., Jin, L., 2018. Summer-winter differences of PM(2.5) toxicity to human alveolar epithelial cells (A549) and the roles of transition metals. *Ecotoxicol. Environ. Saf.* 165, 505–509. <https://doi.org/10.1016/j.ecoenv.2018.09.034>.
- Chen, D., Tang, T.-X., Deng, H., Yang, X.-P., Tang, Z.-H., 2021. Interleukin-7 biology and its effects on immune cells: mediator of generation, differentiation, survival, and homeostasis. *Front. Immunol.* 12, 747324. <https://doi.org/10.3389/fimmu.2021.747324>.
- Costabile, F., Gualtieri, M., Rinaldi, M., Canepari, S., Vecchi, R., Massimi, L., Di Iulio, G., Paglione, M., Di Liberto, L., Corsini, E., Fascini, M.C., Decesari, S., 2023. Exposure to urban nanoparticles at low PM $_{2.5}$  concentrations as a source of oxidative stress and inflammation. *Sci. Rep.* 13, 18616. <https://doi.org/10.1038/s41598-023-45230-z>.
- Daiber, A., Kuntic, M., Hahad, O., Delogu, L.G., Rohrbach, S., Di Lisa, F., Schulz, R., Münzel, T., 2020. Effects of air pollution particles (ultrafine and fine particulate matter) on mitochondrial function and oxidative stress - implications for cardiovascular and neurodegenerative diseases. *Arch. Biochem. Biophys.* 696, 108662. <https://doi.org/10.1016/j.abb.2020.108662>.
- van Eeden, S.F., Tan, W.C., Suwa, T., Mukae, H., Terashima, T., Fujii, T., Qui, D., Vincent, R., Hogg, J.C., 2001. Cytokines involved in the systemic inflammatory response induced by exposure to particulate matter air pollutants (PM $_{10}$ ). *Am. J. Respir. Crit. Care Med.* 164, 826–830. <https://doi.org/10.1164/ajrccm.164.5.2010160>.
- Erin, E.M., Zacharasiewicz, A.S., Nicholson, G.C., Tan, A.J., Higgins, L.A., Williams, T.J., Murdoch, R.D., Durham, S.R., Barnes, P.J., Hansel, T.T., 2005. Topical corticosteroid inhibits interleukin-4, -5 and -13 in nasal secretions following allergen challenge. *Clin. Exp. Allergy J. Br. Soc. Allergy Clin. Immunol.* 35, 1608–1614. <https://doi.org/10.1111/j.1365-2222.2005.02381.x>.
- Faber, S.C., McCullough, S.D., 2018. Through the looking glass: in vitro models for inhalation toxicology and interindividual variability in the airway. *Appl. Vitro. Toxicol.* 4, 115–128. <https://doi.org/10.1089/aivt.2018.0002>.
- George, L., Brightling, C.E., 2016. Eosinophilic airway inflammation: role in asthma and chronic obstructive pulmonary disease. *Ther. Adv. Chronic Dis.* 7, 34–51. <https://doi.org/10.1177/2040622315609251>.
- Gilles, S., Behrendt, H., Ring, J., Traidl-Hoffmann, C., 2012. The pollen enigma: modulation of the allergic immune response by non-allergenic, pollen-derived compounds. *Curr. Pharm. Des.* 18, 2314–2319. <https://doi.org/10.2174/138161212800166040>.
- Gualtieri, M., Grollino, M.G., Consales, C., Costabile, F., Manigrasso, M., Avino, P., Aufderheide, M., Cordelli, E., Di Liberto, L., Petralia, E., Raschella, G., Stracquadanio, M., Wiedensohler, A., Pacchierotti, F., Zanini, G., 2018. Is it the time to study air pollution effects under environmental conditions? A case study to support the shift of in vitro toxicology from the bench to the field. *Chemosphere* 207, 552–564. <https://doi.org/10.1016/j.chemosphere.2018.05.130>.
- Guénette, J., Breznan, D., Thomson, E.M., 2022. Establishing an air-liquid interface exposure system for exposure of lung cells to gases. *Inhal. Toxicol.* 34, 80–89. <https://doi.org/10.1080/08958378.2022.2039332>.
- Hanzalova, K., Rossner, P.J., Sram, R.J., 2010. Oxidative damage induced by carcinogenic polycyclic aromatic hydrocarbons and organic extracts from urban air particulate matter. *Mutat. Res.* 696, 114–121. <https://doi.org/10.1016/j.mrgentox.2009.12.018>.
- Hussain, M., Liu, G., 2024. Eosinophilic asthma: pathophysiology and therapeutic horizons. *Cells* 13. <https://doi.org/10.3390/cells13050384>.

- IARC Working Group on the Evaluation of Carcinogenic Risks to Humans, 2016. *Outdoor Air Pollution, IARC Monographs on the Evaluation of Carcinogenic Risks to Humans. International Agency for Research on Cancer, World Health Organization.*
- Klaunig, J.E., 2018. Oxidative stress and cancer. *Curr. Pharm. Des.* 24, 4771–4778. <https://doi.org/10.2174/1381612825666190215121712>.
- Korbecki, J., Maruszewska, A., Bosiacki, M., Chlubek, D., Baranowska-Bosiacka, I., 2022. The potential importance of CXCL1 in the physiological state and in noncancer diseases of the cardiovascular system, respiratory system and skin. *Int. J. Mol. Sci.* 24. <https://doi.org/10.3390/ijms24010205>.
- Kostova, Z., Batsalova, T., Moten, D., Teneva, I., Dzhabazov, B., 2015. Ragweed-allergic subjects have decreased serum levels of chemokines CCL2, CCL3, CCL4 and CCL5 out of the pollen season. *Cent. -Eur. J. Immunol.* 40, 442–446. <https://doi.org/10.5114/cej.2015.56965>.
- Kumar, S., Joos, G., Boon, L., Tournoy, K., Provoost, S., Maes, T., 2017. Role of tumor necrosis factor- $\alpha$  and its receptors in diesel exhaust particle-induced pulmonary inflammation. *Sci. Rep.* 7, 11508. <https://doi.org/10.1038/s41598-017-11991-7>.
- Libalová, H., Závodná, T., Vrbová, K., Sikorová, J., Vojtisek-Lom, M., Beránek, V., Pechout, M., Kléma, J., Ciganek, M., Machala, M., Neča, J., Rössner, P.J., Topinka, J., 2021. Transcription profiles in BEAS-2B cells exposed to organic extracts from particulate emissions produced by a port-fuel injection vehicle, fueled with conventional fossil gasoline and gasoline-ethanol blend. *Mutat. Res. Genet. Toxicol. Environ. Mutagen.* 872, 503414. <https://doi.org/10.1016/j.mrgentox.2021.503414>.
- Lin, Shouheng, Zhang, X., Huang, G., Cheng, L., Lv, J., Zheng, D., Lin, Simiao, Wang, S., Wu, Q., Long, Y., Li, B., Wei, W., Liu, P., Pei, D., Li, Y., Wen, Z., Cui, S., Li, P., Sun, X., Wu, Y., Yao, Y., 2021. Myeloid-derived suppressor cells promote lung cancer metastasis by CCL11 to activate ERK and AKT signaling and induce epithelial-mesenchymal transition in tumor cells. *Oncogene* 40, 1476–1489. <https://doi.org/10.1038/s41388-020-01605-4>.
- Lujan, H., Crisciello, M.F., Hering, A.S., Sayes, C.M., 2019. Refining in vitro toxicity models: comparing baseline characteristics of lung cell types. *Toxicol. Sci. Off. J. Soc. Toxicol.* 168, 302–314. <https://doi.org/10.1093/toxsci/kfz001>.
- Määttä, J., Majuri, M.-L., Luukkonen, R., Lauerma, A., Husgafvel-Pursiainen, K., Alenius, H., Savolainen, K., 2005. Characterization of oak and birch dust-induced expression of cytokines and chemokines in mouse macrophage RAW 264.7 cells. *Toxicology* 215, 25–36. <https://doi.org/10.1016/j.tox.2005.06.021>.
- Mukhopadhyay, S., Hoidal, J.R., Mukherjee, T.K., 2006. Role of TNF $\alpha$  in pulmonary pathophysiology. *Respir. Res.* 7, 125. <https://doi.org/10.1186/1465-9921-7-125>.
- Pan, R., Kuai, S., Li, Q., Zhu, X., Wang, T., Cui, Y., 2023. Diagnostic value of IL-6 for patients with asthma: a meta-analysis. *Allergy Asthma Clin. Immunol. Off. J. Can. Soc. Allergy Clin. Immunol.* 19, 39. <https://doi.org/10.1186/s13223-023-00794-3>.
- Peters, M.C., Mauger, D., Ross, K.R., Phillips, B., Gaston, B., Cardet, J.C., Israel, E., Levy, B.D., Phipatanakul, W., Jarjour, N.N., Castro, M., Wenzel, S.E., Hastie, A., Moore, W., Bleecker, E., Fahy, J.V., Denlinger, L.C., 2020. Evidence for exacerbation-prone asthma and predictive biomarkers of exacerbation frequency. *Am. J. Respir. Crit. Care Med.* 202, 973–982. <https://doi.org/10.1164/rccm.201909-1813OC>.
- Pozzer, A., Anenberg, S.C., Dey, S., Haines, A., Lelieveld, J., Chowdhury, S., 2023. Mortality attributable to ambient air pollution: a review of global estimates. *e2022GH000711 GeoHealth* 7. <https://doi.org/10.1029/2022GH000711>.
- Puxeddu, I., Bader, R., Piliposky, A.M., Reich, R., Levi-Schaffer, F., Berkman, N., 2006. The CC chemokine eotaxin/CCL11 has a selective profibrogenic effect on human lung fibroblasts. *J. Allergy Clin. Immunol.* 117, 103–110. <https://doi.org/10.1016/j.jaci.2005.08.057>.
- Qi, X., Huang, J., Zhang, T., Han, Z., Wang, Y., Sun, Y., Hou, L., Li, X., Lei, W., Bai, L., Xing, Y., Wang, J., Junling, P., Wang, C., 2024. Unveiling CXCL12/CXCR4 Axis as a Common Pathway in Diverse Types of Pulmonary Fibrosis and the Therapeutic Potential of Plerixafor.
- Rahmatinia, T., Kermani, M., Farzadkia, M., Jonidi Jafari, A., Delbandi, A.-A., Rashidi, N., Fanaei, F., 2022. The effect of PM(2.5)-related hazards on biomarkers of bronchial epithelial cells (A549) inflammation in Karaj and Fardis cities. *Environ. Sci. Pollut. Res. Int.* 29, 2172–2182. <https://doi.org/10.1007/s11356-021-15723-3>.
- Reibman, J., Hsu, Y., Chen, L.C., Kumar, A., Su, W.C., Choy, W., Talbot, A., Gordon, T., 2002. Size fractions of ambient particulate matter induce granulocyte macrophage colony-stimulating factor in human bronchial epithelial cells by mitogen-activated protein kinase pathways. *Am. J. Respir. Cell Mol. Biol.* 27, 455–462. <https://doi.org/10.1165/rcmb.2001-0005OC>.
- Roffel, M.P., Bracke, K.R., Heijink, I.H., Maes, T., 2020. miR-223: A Key Regulator in the Innate Immune Response in Asthma and COPD. *Front. Med.* 7, 196. <https://doi.org/10.3389/fmed.2020.00196>.
- Rossner, P.J., Cervena, T., Vojtisek-Lom, M., 2021. In vitro exposure to complete engine emissions - a mini-review. *Toxicology* 462, 152953. <https://doi.org/10.1016/j.tox.2021.152953>.
- Rossner, P.J., Cervena, T., Vojtisek-Lom, M., Vrbova, K., Ambroz, A., Novakova, Z., Elzeinova, F., Margaryan, H., Beranek, V., Pechout, M., Macoun, D., Klema, J., Rossnerova, A., Ciganek, M., Topinka, J., 2019. The biological effects of complete gasoline engine emissions exposure in a 3D human airway model (MucilAir(TM)) and in human bronchial epithelial cells (BEAS-2B). *Int. J. Mol. Sci.* 20. <https://doi.org/10.3390/ijms20225710>.
- Rossner, P.J., Svecova, V., Schmutzerova, J., Milcova, A., Tabashidze, N., Topinka, J., Pastorkova, A., Sram, R.J., 2013. Analysis of biomarkers in a Czech population exposed to heavy air pollution. Part I: bulky DNA adducts. *Mutagenesis* 28, 89–95. <https://doi.org/10.1093/mutage/ges057>.
- Rossner, P.J., Tulupova, E., Rossnerova, A., Libalova, H., Honkova, K., Gmuender, H., Pastorkova, A., Svecova, V., Topinka, J., Sram, R.J., 2015. Reduced gene expression levels after chronic exposure to high concentrations of air pollutants. *Mutat. Res.* 780, 60–70. <https://doi.org/10.1016/j.mrfmmm.2015.08.001>.
- Salvi, S.S., Nordenhall, C., Blomberg, A., Rudell, B., Pourazar, J., Kelly, F.J., Wilson, S., Sandström, T., Holgate, S.T., Frew, A.J., 2000. Acute exposure to diesel exhaust increases IL-8 and GRO- $\alpha$  production in healthy human airways. *Am. J. Respir. Crit. Care Med.* 161, 550–557. <https://doi.org/10.1164/ajrccm.161.2.9905052>.
- Santoro, M., Costabile, F., Gualtieri, M., Rinaldi, M., Paglione, M., Busetto, M., Di Iulio, G., Di Liberto, L., Gherardi, M., Pelliccioni, A., Monti, P., Barbara, B., Grollino, M.G., 2024. Associations between fine particulate matter, gene expression, and promoter methylation in human bronchial epithelial cells exposed within a classroom under air-liquid interface. *Environ. Pollut.* 358, 124471. <https://doi.org/10.1016/j.envpol.2024.124471>.
- Takizawa, H., Abe, S., Okazaki, H., Kohyama, T., Sugawara, I., Saito, Y., Ohtoshi, T., Kawasaki, S., Desaki, M., Nakahara, K., Yamamoto, K., Matsushima, K., Tanaka, M., Sagai, M., Kudoh, S., 2003. Diesel exhaust particles upregulate eotaxin gene expression in human bronchial epithelial cells via nuclear factor-kappa B-dependent pathway. *Am. J. Physiol. Lung Cell. Mol. Physiol.* 284, L1055–L1062. <https://doi.org/10.1152/ajplung.00358.2002>.
- Tsai, D.-H., Amyai, N., Marques-Vidal, P., Wang, J.-L., Riediker, M., Mooser, V., Paccaud, F., Waeber, G., Vollenweider, P., Bochud, M., 2012. Effects of particulate matter on inflammatory markers in the general adult population. *Part Fibre Toxicol.* 9, 24. <https://doi.org/10.1186/1743-8977-9-24>.
- Uciechowski, P., Dempke, W.C.M., 2020. Interleukin-6: a masterplayer in the cytokine network. *Oncology* 98, 131–137. <https://doi.org/10.1159/000505099>.
- Vizuete, W., Sexton, K.G., Nguyen, H., Smeester, L., Aagaard, K.M., Shope, C., Lefer, B., Flynn, J.H., Alvarez, S., Erickson, M.H., Fry, R.C., 2015. From the field to the laboratory: air pollutant-induced genomic effects in lung cells. *Environ. Health Insights* 9, 15–23. <https://doi.org/10.4137/EHI.S15656>.
- Vojtisek-Lom, M., Pechout, M., Macoun, D., Rameswaran, R., Prahara, K., Cervena, T., Topinka, J., Rossner, P., 2019. Assessing exhaust toxicity with biological detector: configuration of portable air-liquid interface human lung cell model exposure system, sampling train and test conditions. *SAE Int. J. Adv. Curr. Pract. Mobil.* <https://doi.org/10.4271/2019-24-0050>.
- Wahlina, P., Palmgren, F., Van Dingenen, R., 2001. Experimental studies of ultrafine particles in streets and the relationship to traffic. *Atmos. Environ.* 35, S63–S69. [https://doi.org/10.1016/S1352-2310\(00\)00500-8](https://doi.org/10.1016/S1352-2310(00)00500-8).
- Wang, R., Chen, R., Wang, Y., Chen, L., Qiao, J., Bai, R., Ge, G., Qin, G., Chen, C., 2019. Complex to simple: In vitro exposure of particulate matter simulated at the air-liquid interface discloses the health impacts of major air pollutants. *Chemosphere* 223, 263–274. <https://doi.org/10.1016/j.chemosphere.2019.02.022>.
- Wu, X., Qian, L., Zhao, H., Lei, W., Liu, Y., Xu, X., Li, J., Yang, Z., Wang, D., Zhang, Yuchen, Zhang, Yan, Tang, R., Yang, Y., Tian, Y., 2023. CXCL12/CXCR4: an amazing challenge and opportunity in the fight against fibrosis. *Ageing Res. Rev.* 83, 101809. <https://doi.org/10.1016/j.arr.2022.101809>.
- Yatera, K., Nishida, C., 2024. Contemporary concise review 2023: environmental and occupational lung diseases. *Respirology* 29, 574–587. <https://doi.org/10.1111/resp.14761>.
- Zhou, Z., Liu, Y., Duan, F., Qin, M., Wu, F., Sheng, W., Yang, L., Liu, J., He, K., 2015. Transcriptomic analyses of the biological effects of airborne PM2.5 exposure on human bronchial epithelial cells. *PLoS One* 10, e0138267. <https://doi.org/10.1371/journal.pone.0138267>.